Cell Tissue Res (2014) 356:391–403
DOI 10.1007/s00441-014-1801-4

REGULAR ARTICLE

Expansion on a matrix deposited by nonchondrogenic urine stem cells strengthens the chondrogenic capacity of repeated-passage bone marrow stromal cells

Ming Pei · Jingting Li · Ying Zhang · Guihua Liu · Lei Wei · Yuanyuan Zhang

Received: 1 September 2013 / Accepted: 9 January 2014 / Published online: 6 April 2014

Abstract Human urine-derived stem cells (hUSCs) are a newly found type of stem cell with a potential for therapeutic application in urology. The aim of this study is to investigate whether hUSCs contribute to cartilage regeneration. Despite their characterization with multi-lineage differentiation capacities, in terms of osteogenesis, adipogenesis and myogenesis, hUSCs do not show the ability to differentiate into chondrocytes. Human bone marrow stromal cells (hBMSCs) are a tissue-specific stem cell for endochondral bone formation; however, repeated-passage hBMSCs have a lower capacity for chondrogenic differentiation. We found that the extracellular matrix (ECM) deposited by hUSCs (UECM) can greatly recharge repeated-passage hBMSCs toward chondrogenic differentiation, a result that might be explained by trophic factors released from hUSCs being immobilized in UECM. We also found that ECM from repeated-passage hBMSCs (BECM) have a limited rejuvenation effect. The Wnt11-mediated noncanonical signaling pathway might be responsible for UECM-mediated hBMSC rejuvenation and subsequent chondrogenic differentiation. Our data indicate that commercially available UECM from young healthy donors might represent a simple and promising approach for autologous hBMSC rejuvenation. This study also provides an excellent model for investigating the effect of trophic factors released by stem cells on tissue regeneration without interference by stem cell differentiation.

Keywords Decellularized stem cell matrix · Monolayer expansion · Urine-derived stem cells · Bone marrow stromal cells · Endochondral bone formation · Human

This project was partially supported by research grants from the West Virginia University Senate Research Grant Award (R-12-010), the AO Foundation (S-12-19P), the Musculoskeletal Transplant Foundation and NIH R03 (no. 1 R03 AR062763-01A1 and no. 5 R03 DE021433-02).

M. Pei (✉) · J. Li · Y. Zhang
Stem Cell and Tissue Engineering Laboratory, Department of Orthopaedics, West Virginia University, PO Box 9196, One Medical Center Drive, Morgantown, WV 26506-9196, USA
e-mail: mpei@hsc.wvu.edu

M. Pei · J. Li
Exercise Physiology, West Virginia University, Morgantown, WV 26506, USA

M. Pei · Y. Zhang
Mechanical & Aerospace Engineering, West Virginia University, Morgantown, WV 26506, USA

G. Liu · Y. Zhang
Wake Forest Institute for Regenerative Medicine, Winston-Salem, NC 27157, USA

L. Wei
Molecular Biology Laboratory, Department of Orthopaedics, Alpert Medical School of Brown University, Providence, RI 02903, USA

Introduction

Cell-therapy-based bone tissue engineering is a promising biological treatment for large bone defects. Increasing evidence indicates that the engineering of hypertrophic cartilage templates as bone substitute materials is a suitable novel approach for bone regeneration via endochondral ossification, an in vitro imitation of the embryonic developmental pathway of long bones and the axial skeleton (Kronenberg 2003). Autologous bone regeneration can avoid immune rejection and disease transmission. The identification of an appropriate adult stem cell that is capable not only of chondrogenic differentiation but also of ending in hypertrophy is therefore critical. Under chondrogenic induction, synovium-derived stem cells, a tissue-specific stem cell type for chondrogenesis, have a reduced tendency to become hypertrophic (Jones and Pei 2012; Pei et al. 2008a, b); in contrast, bone marrow

stromal cells (BMSCs) show not only chondrogenic potential but also a 5- to 10-fold increase in osteocalcin and alkaline phosphatase activity (Djouad et al. 2005), indicating that BMSCs are a promising tissue-specific stem cell for endochondral bone formation (Pei et al. 2011a).

The search for an appropriate stem cell for tissue-specific lineage differentiation is the first step in successful lineage-specific tissue regeneration. Because of the limited colony-forming potential of nucleated cells in BMSCs (1 in 1,000–10,000; Jo et al. 2007), large-scale cell expansion is needed; however, conventional cell expansion (monolayer culture) results in cell senescence in terms of the loss of cell proliferation and differentiation capacity (Li and Pei 2012). Our previous findings have suggested that the decellularized stem cell matrix is an excellent cell expansion system for stem cell rejuvenation in cartilage engineering and regeneration (Pei et al. 2011b). Despite the finding that early passage human BMSCs (hBMSCs) can be rejuvenated when expanded on their own extracellular matrix (ECM; Pei et al. 2011a), our preliminary data have shown that repeated-passage stem cells might not be rejuvenated by ECM deposited by such senescent stem cells.

Recently, a subpopulation of cells isolated from urine, termed urine-derived stem cells (USCs), has been found to possess biological characteristics similar to those of mesenchymal stem cells (MSCs), i.e., clonogenicity, cell growth patterns, expansion capacity, multi-lineage differentiation capacity, pro-angiogenic paracrine effects and immunomodulatory properties (Liu et al. 2013; Zhang et al. 2008). Since human USCs (hUSCs) can be collected by using a simple, safe, low-cost, and non-invasive procedure, this type of stem cell from young healthy donors can be used as a potential cell source for the preparation of commercially available ECM.

In this study, we were curious about whether hUSCs could be a potential stem cell source for cartilage regeneration; we also wondered whether ECM deposited by hUSCs could provide an immobilized trophic stimulation for late-passage hBMSC rejuvenation. Because Wnt signaling is a critical pathway in the regulation of chondrogenesis and cartilage development (Yates et al. 2005), we assessed the change in Wnt signals in the ECM-mediated hBMSC chondrogenic differentiation.

Materials and methods

Cell culture

Human BMSCs were purchased from Lonza Group (Basel, Switzerland) and pooled from five donors (20–43 years old, average: 25 years old; three males and two females), as described in our previous study (Pei et al. 2011a). Human USCs were donated by Wake Forest University and approved for this study by the Institutional Review Board. The isolation of hUSCs was described in a previous study (Zhang et al. 2008). Briefly, urine samples were collected from four healthy male individuals. Each urine sample was centrifuged at 500*g* for 5 min to collect cells. Both BMSCs and USCs were cultured in growth medium (alpha minimum essential medium; αMEM; Invitrogen, Carlsbad, Calif., USA) containing 10 % fetal bovine serum (FBS), 100 U/ml penicillin, 100 μg/ml streptomycin and 0.25 μg/ml fungizone.

USC characterization

Population doubling and doubling time

Human USC cell number and culture time were counted at each passage from passage 0 onwards. Population doubling (PD) and doubling time (DT) were calculated by using the following formula: $PD=\ln(N_f/N_i)/\ln(2)$; $DT=C_t/PD$ (N_f: final number of cells, N_i: initial number of cells, C_t: culture time)

Flow cytometry analysis

Human USCs at passage 2 were stained with specific anti-human antibodies labeled with CD14-allophycocyanin (APC), CD24-fluorescein-isothiocyanate (FITC), CD29-phycoerythrin (PE), CD31-FITC, CD34-APC, CD44-PE, CD45-APC, CD73-APC, CD90-APC, CD105-PE, CD117-PE, CD133-PE, CD146-PE, SSEA-4-PE, and STRO-1-FITC (Table 1). Briefly, trypsinized hUSCs (5×10^5) were re-suspended in ice-cold phosphate-buffered saline (PBS) containing 1 % bovine serum albumin (BSA). Fluorochrome-conjugated antibodies were added to cells in 50 μl PBS containing 3 % BSA and incubated on ice for 30 min in the dark. IgG1-PE, IgG1-FITC and IgG1-APC-conjugated isotype control antibodies were used to subtract background fluorescence. After being filtered through a 70-μm cell strainer, cells were analyzed by using flow cytometry (FACS Calibur, BD Biosciences, Franklin Lakes, N.J., USA) and FlowJo software (TreeStar, Ashland, Ore., USA).

Enzyme-linked immunosorbent assay plate array

A total of 2×10^5 hUSCs at passage 2 were seeded in a six-well plate and then incubated with serum-free αMEM at 37 °C in 5 % CO_2 for 24 h. The conditioned medium was collected and analyzed by human cytokine enzyme-linked immunosorbent assay (ELISA) plate array (Signosis, Sunnyvale, Calif., USA) according to the manufacturer's instructions. Briefly, 100 μl culture supernatant was incubated in 96-well plates on a rocking platform at room temperature for 1 h. After incubation with the detection antibody mixture, the plates were measured with chemiluminescent substrate by a luminometer plate reader for relative light unit (RLU).

Table 1 Antibodies used in flow cytometry analysis (*APC* allophycocyanin, *FITC* fluorescein-isothiocyanate, *PE* phycoerythrin)

Antibodies	Source Ig	Against	Company catalog number
CD14-APC	Mouse IgG1	Human	R&D system FAB3832A
CD24-FITC	Mouse IgG2a, κ	Human	BD 560992
CD29-PE	Mouse IgG1, κ	Human	BD 555443
CD29-PE	Mouse IgG2a, κ	Human	BD 556049
CD31-FITC	Mouse IgG1, κ	Human	BD 560984
CD34-FITC	Mouse IgG	Human	BD 348053
CD44-PE	Mouse IgG1, κ	Human	BD 550989
CD45-APC	Mouse IgG1	Human	BD 340943
CD73-PE	Mouse IgG1, κ	Human	BD 550257
CD90-APC	Mouse IgG1, κ	Human	BD 559869
CD105-PE	Mouse IgG1, κ	Human	BD 560839
CD117-PE	Mouse IgG 1	Human	BD 340867
CD133-PE	Mouse IgG1	Human	MACS 130080801
CD146-PE	Mouse IgG1, κ	Human	BD 550315
STRO-FITC	Mouse IgM, l	Human	Biolegend 340105
SSEA-4-PE	Mouse IgG3, κ	Human	BD 560128
MsIgG1-PE	Mouse IgG1, κ		BD 559320
MsIgG1-FITC	Mouse IgG1, κ		BD 555909
MsIgG1-APC	Mouse IgG1, κ		BD 555751

Multi-lineage differentiation

Osteogenic induction hUSCs were seeded at a density of 4000 cells/cm^2 and incubated in an osteogenic induction medium containing low-glucose Dulbecco's modified Eagle's medium (DMEM) with 100 nM dexamethasone, 10 mM β-glycerophosphate and 50 mM ascorbic acid-2-phosphate (Wako Chemicals, Richmond, Va., USA) for 28 days. Osteogenic differentiation was assessed by using Alizarin Red S staining (ARS) as described previously (Pei et al. 2011a; Li et al. 2012).

Adipogenic induction hUSCs were seeded at a density of 4000 cells/cm^2 and cultured in an adipogenic induction medium containing low-glucose DMEM with 1 μM dexamethasone, 500 μM 3-isobutyl-1-methylxanthine, 10 μg/ml insulin and 100 μM indomethacin for 28 days. Adipogenic differentiation was assessed by using Oil Red O staining (ORO) as described previously (Pei et al. 2011a; Li et al. 2012).

Smooth muscle cell induction hUSCs were plated at 2000 cells/cm^2 in smooth muscle differentiation media containing equal amounts of high-glucose DMEM and embryonic fibroblast medium (EFM) with 10 % FBS, 2.5 ng/ml transforming growth factor beta1 (TGF-β1) and 5 ng/ml platelet-derived growth factor BB (PDGF-BB; R&D Systems, Minneapolis, Minn., USA). Cell morphology was recorded before and after growth factor additions for up to 14 days. The slides were fixed with freshly prepared 4 % paraformaldehyde for 20 min followed by permeabilization with 0.1 % Triton-X100 in PBS for 10 min and blocked with serum-free block solution (Dako, Denmark) for 15 min. Lineage-specific primary antibodies, namely rabbit polyclonal antibodies to desmin (abcam, Cambridge, Mass. USA; catalog number ab15200) and MyoD (C-20, Santa Cruz Biotechnology, Dallas, Tex., USA; catalog number sc-304), were incubated at 4 °C overnight followed by secondary antibody conjugated to Alexa Fluor 594 (Life Technologies, Grand Island, N.Y., USA; catalog number A11072) for 30 min in the dark. The slides were mounted by using anti-fade mounting media (Vector Laboratories, Burlingame, Calif., USA) containing propidium iodide (PI) and images were captured by using a Leica upright microscope (DM 4000B, Wetzlar, Germany).

ECM preparation

Passage 3 hUSCs and passage 8 hBMSCs were used to prepare ECM, termed UECM and BECM, respectively, as described in our previous study (Pei et al. 2011a; He et al. 2009). Briefly, when the cells seeded on plastic flasks (Plastic) reached 90 % confluence, 50 μM L-ascorbic acid phosphate (Wako Chemicals USA) was added for 8 days. The deposited matrix was incubated with 0.5 % Triton X-100 containing 20 mM ammonium hydroxide at 37 °C for 5 min and stored at 4 °C in PBS containing 100 U/ml penicillin, 100 μg/ml streptomycin and 0.25 μg/ml fungizone.

Human USC-derived ECM characterization

Scanning electron microscopy

Representative samples (n=2) were primarily fixed in 2.5 % glutaraldehyde for 2 h followed by secondary fixation in 2 % osmium tetroxide as described previously (Tan et al. 2010). The samples were then dehydrated consecutively in 25 %, 50 %, 75 %, 95 % and 100 % ethanol for 10 min each, in hexamethyldisilazane (HMDS) at a ratio of 1:1 with ethanol twice for 1 h each time, in HMDS at a ratio of 1:2 with ethanol overnight and in HMDS three times for 4 h each time. The samples were air-dried for 24 h and gold-sputtered. The images were recorded by a scannng electron microscope (Model S 2400; Hitachi, Brisbane, Calif., USA).

Immunofluorescent staining

ECM was fixed with 4 % paraformaldehyde in PBS for 30 min. After incubation in 10 % normal goat serum for 1 h, ECM was treated with mouse monoclonal antibodies to type I collagen (Clone COL1, Sigma-Aldrich, St. Louis, Mo., USA; catalog number C2456), fibronectin (EP5, Santa Cruz Biotechnology; catalog number sc-8422) and laminin 5 (P3E4,

Santa Cruz Biotechnology; catalog number sc-13587) at 4 °C overnight, followed by incubation in Alexa Fluor 488 goat anti-mouse IgG (Life Technologies) for 30 min.

Expanded cell chondrogenic induction and evaluation

Passage 3 hUSCs and passage 8 hBMSCs were expanded on plastic, UECM, or BECM for one passage. Upon reaching confluence, the expanded cells (3×10^5 cells) were centrifuged to form a pellet. After overnight incubation (day 0), the pellets were cultured in a serum-free chondrogenic medium consisting of high-glucose DMEM, 40 μg/ml proline, 100 nM dexamethasone, 100 U/ml penicillin, 100 μg/ml streptomycin, 0.1 mM ascorbic acid-2-phosphate and 1× ITS Premix (BD Biosciences) plus supplementation with 10 ng/ml TGF-β3 (PeproTech, Rocky Hill, N.J., USA) in a 5 % O_2 and 5 % CO_2 incubator for 14 days.

Histology and immunostaining

The pellets (n=3) were fixed in 4 % paraformaldehyde at 4 °C overnight, followed by being dehydrated in a gradient ethanol series, cleared with xylene and embedded in paraffin blocks. Sections (5 μm thick) were stained with Alcian blue (counterstained with fast red) for sulfated glycosaminoglycans (GAGs). The sections were also immunolabeled with primary antibodies against type II collagen (Developmental Studies Hybridoma Bank, Iowa City, Iowa, USA; catalog number II-II6B3) and type X collagen (Sigma-Aldrich; catalog number C7974), followed by the secondary antibody, namely biotinylated horse anti-mouse IgG (Vector Laboratories). Immunoactivity was detected by using Vectastain ABC reagent (Vector Laboratories) with 3,3′-diaminobenzidine as a substrate.

Biochemical analysis

The pellets (n=4) were digested at 60 °C for 4 h with 125 μg/ml papain in PBE buffer (100 mM phosphate and 10 mM ethylenediaminetetraacetic acid, pH 6.5) containing 10 mM cysteine. The amount of DNA in the papain digestion was measured by using the QuantiT PicoGreen dsDNA assay kit (Invitrogen) with a CytoFluor Series 4000 (Applied Biosystems, Foster City, Calif., USA). GAG was measured by using dimethylmethylene blue dye and a Spectronic BioMate 3 Spectrophotometer (Thermo Scientific, Milford, Mass., USA) with bovine chondroitin sulfate as a standard.

Taqman real-time polymerase chain reaction

Total RNA was extracted from samples (n=4) by using an RNase-free pestle in TRIzol (Invitrogen). About 1 μg mRNA was used for reverse transcription with a High-Capacity cDNA Archive Kit (Applied Biosystems) at 37 °C for 120 min. Chondrogenic marker genes [type II collagen (*COL2A1*) and aggrecan (*ACAN*)] and a hypertrophic marker gene [type X collagen (*COL10A1*)] were customized by Applied Biosystems as part of their Custom TaqMan Gene Expression Assays (Pei et al. 2013). Eukaryotic 18S RNA (Assay ID HS99999901_s1) was used as the endogenous control. Real-time polymerase chain reaction (PCR) was performed with the iCycler iQ Multi-Color Real Time PCR Detection (Perkin-Elmer, Waltham, Mass., USA). Relative transcript levels were calculated as $\chi=2^{-\Delta\Delta Ct}$, in which $\Delta\Delta Ct=\Delta E-\Delta C$, $\Delta E=Ct_{exp}-Ct_{18s}$ and $\Delta C=Ct_{ct1}-Ct_{18s}$.

Western blot

To determine potential mechanisms underlying ECM-mediated cell chondrogenic differentiation further, the pellets from expanded hBMSCs were homogenized on dry ice and dissolved in lysis buffer (Cell Signaling, Danvers, Mass., USA) with protease inhibitors. Total proteins were quantified by using the BCA Protein Assay Kit (Thermo Fisher Scientific, Waltham, Mass., USA). Protein (30 μg) from each sample was denatured and separated by using NuPAGE Novex Bis-TRIS Mini Gels (Invitrogen) in the XCell SureLock Mini-Cell (Invitrogen) at 120 V at 4 °C for 3 h. Bands were transferred onto a nitrocellulose membrane (Invitrogen) by using an XCell II Blot Module (Invitrogen) at 15 V at 4 °C overnight. The membrane was incubated with primary monoclonal antibodies in 5 % BSA, 1×TBS (10 mM TRIS–HCl, 150 mM NaCl, pH 7.5) and 0.05 % Tween-20 at room temperature for 1 h (β-actin served as an internal control), followed by the secondary antibody, namely horseradish-peroxidase–conjugated goat anti-mouse (Thermo Fisher Scientific) for 1 h. SuperSignal West Femto Maximum Sensitivity Substrate (Thermo Fisher Scientific) and CL-XPosure Film (Thermo Fisher Scientific) were used for exposure. The primary antibodies used in immunoblotting included the Wnt3a (C64F2) monoclonal antibody (Cell Signaling; catalog number 2721), Wnt5a monoclonal antibody (Cell Signaling; catalog number 2530) and Wnt11 polyclonal antibody (Thermo Fisher Scientific; catalog number PIPA521712).

Statistical analysis

Numerical data are presented as the means and standard error of the mean. The Mann–Whitney U test was used for pairwise comparison in biochemistry and real-time PCR data analysis. All statistical analyses were performed with SPSS 13.0 statistical software (SPSS, Chicago, Ill. USA). P-values less than 0.05 were considered statistically significant.

Results

Characterization of hUSCs

We determined whether hUSCs exhibited MSC surface phenotypes by flow cytometry. The obtained data showed that hUSCs were strongly positive for typical MSC markers, such as CD24 (heat stable antigen, HSA), CD29 (integrin β1), CD44 (hyaluronan receptor), CD73 (SH3/4), CD90 (Thy-1), CD146 (melanoma cell adhesion molecule, MCAM) and SSEA-4 (stage-specific embryonic antigen 4; Fig. 1ai). CD105 (SH2 and endoglin), CD133 (prominin 1) and STRO-1 (Fig. 1aii) were weak. Monocyte/macrophage markers such as CD14, endothelial markers such as CD31 (platelet endothelial cell adhesion molecule, PECAM-1) and hematopoietic stem cell markers such as CD34 and CD45 (Fig. 1aiii) were negative.

To evaluate whether hUSCs had MSC proliferation capacity, we measured PD and DT for hUSC populations. Our data indicated that the average PD from passage 0 to passage 8 of hUSCs was 61.97±4.80 and the average DT was 27.02± 12.82 h. To determine whether hUSCs had multi-lineage differentiation potentials, hUSCs were incubated in either osteogenic or adipogenic induction medium for 28 days. Osteogenically differentiated hUSCs appeared to produce mineralized tissue demonstrated by Alizarin Red S staining for calcium deposition (Fig. 1b). Adipogenically differentiated hUSCs were positive for Oil Red O staining (Fig. 1c). Additionally, when hUSCs were cultured in myogenic differentiation medium for 14 days, they became elongated and spindle-shaped; immunostaining by desmin (Fig. 1d) and nuclear staining with antibodies to MyoD (Fig. 1e) revealed the myogenic differentiated populations.

To determine whether the supernatant of hUSCs contained trophic factors, a human cytokine ELISA plate array was used to measure the abundance of 31 human cytokines simultaneously (Fig. 1f). Our data suggested that the cytokines secreted by hUSCs included Adipo (adipokines), b-FGF (basic fibroblast growth factor), b-NGF (beta-nerve growth factor), EGF (epidermal growth factor), G-CSF (granulocyte colony-stimulating factor), GM-CSF (granulocyte/macrophage colony-stimulating factor), IFNγ (interferon-gamma), IL-1α (interleukin-1 alpha), IL-2, IL-4, IL-8 (CXCL8), IL-10, IL-12, IL-13, IP-10 (gamma-interferon-inducible protein 10, CXCL10), leptin, MCP-1 (monocyte chemoattractant protein 1, CCL2), MIP-1α (macrophage inflammatory protein-1 alpha, CCL3), PAI-1 (plasminogen activator inhibitor-1), PDGF-BB, PLGF (placenta growth factor-1), resistin, TGF-b, TNFα (tumor necrosis factor alpha) and VEGF (vascular endothelial growth factor); the undetectable factors included Eotaxin-3 (CCL26), IGF-I (insulin-like growth factor I), IL-6, IL-17a, Rantes (regulated on activation, normal T cell expressed and secreted; CCL5) and SCF (stem cell factor).

Physicochemical properties of UECM

To observe the morphology of UECM, hUSCs were used to secrete matrix followed by chemical treatment to remove hUSCs. Data obtained by scanning electron microscopy showed that UECM consisted of matrix fibers and "inter" holes (Fig. 2a); hBMSCs grown on UECM exhibited a fibroblast-like shape (Fig. 2b). To determine the chemical composition of UECM, immunostaining was used to detect three main matrix proteins: collagen, fibronectin and laminin. Our data clearly showed that UECM fibers consisted of type I collagen (Fig. 2c) and fibronectin (Fig. 2d) rather than laminin 5 (Fig. 2e).

hUSCs are not an appropriate stem cell source for chondrogenesis

Compared with the fibroblast-like shape of hBMSCs (Fig. 2f-h), hUSCs exhibited a glistening cobblestone appearance (Fig. 2i-k). When expanded cells were chondrogenically induced, hUSC pellets from both UECM (UonU) and BECM (UonB) expansion gradually became tiny and then disappeared. Compared with those from hBMSCs expanded on corresponding substrates, namely on plastic (BonP; Fig. 3b, f), on BECM (BonB; Fig. 3c, g) and on UECM (BonU; Fig. 3d, h), the pellets from hUSCs expanded on plastic (UonP) were the smallest in size (Fig. 3a, e) with non-detectable chondrogenic expression at either the protein level (Fig. 3a-d: sulfated GAGs; Fig. 3e-h: type II collagen; Fig. 3j: ratio of GAG to DNA) or the mRNA level (Fig. 3k: *ACAN*; Fig. 3l: *COL2A1*), despite surviving a 14-day chondrogenic induction.

ECM deposited by repeated-passage hBMSCs shows decreased rejuvenation ability

Despite no evident difference in chondrogenic differentiation markers of expanded cells on either BECM (Fig. 3c, g) or plastic (Fig. 3b, f), data from the biochemical analysis suggested that hBMSCs expanded on plastic (BonP) yielded pellets with a lower GAG amount compared with those grown on BECM (BonB; data not shown). Even though hBMSCs grown on BECM (BonB) yielded pellets with a higher cell viability (DNA ratio adjusted by day 0; Fig. 3i), no significant difference was seen between the chondrogenic indices (GAG/DNA) of hBMSC pellets from plastic (BonP) and BECM (BonB) expansion (Fig. 3j). Although hBMSCs grown on BECM yielded pellets with higher *ACAN* (Fig. 3k) and *COL2A1* (Fig. 3l) compared with those plated on plastic, our hypertrophy data revealed no significant difference in type X collagen immunostaining (Fig. 4a-d) and *COL10A1* mRNA level (Fig. 4e), indicating that BECM expansion in this study had less rejuvenation effect on hBMSC endochondral

ossification compared with a previous study (Pei et al. 2011a); replicative senescence from ECM deposited by the cells was possibly a major factor.

ECM deposited by hUSCs preconditions hBMSCs for chondrogenic hypertrophy

Surprisingly, passage 8 hBMSCs expanded on UECM exhibited a strongly enhanced chondrogenic potential, as evidenced by an impressively large pellet size with intensified staining of sulfated GAGs (Fig. 3d) and type II collagen (Fig. 3h). These results were supported by biochemical data in which hBMSCs expanded on UECM (BonU) yielded pellets with the highest GAG amount and chondrogenic index (Fig. 3j) and by real-time PCR data in which hBMSCs grown on UECM (BonU) yielded pellets with the highest mRNA levels of *ACAN* (Fig. 3k) and *COL2A1* (Fig. 3l). Interestingly, chondrogenic hypertrophy was concomitantly promoted, as evidenced by immunostaining for type X collagen (Fig. 4a-d) and real-time PCR for *COL10A1* mRNA (Fig. 4e). The above data indicate that expansion on UECM strengthens the chondrogenic capacity of repeated-passage hBMSCs.

Involvement of Wnt11-mediated noncanonical signaling pathway in the rejuvenation of hBMSCs by UECM

To determine whether Wnt signals were regulated during the chondrogenic differentiation of hBMSCs after expansion on various substrates, Western blot was used to detect Wnt3a (a typical activator for canonical Wnt signaling), Wnt5a and Wnt11 (both being typical activators for noncanonical Wnt signaling) in hBMSC pellets at day 0 (24 h after forming a pellet but before chondrogenic induction), day 7 (early stage of chondrogenic induction) and day 14 (late stage of chondrogenic induction). Our data suggested that, under chondrogenic induction, both Wnt3a (Fig. 5a) and Wnt5a (Fig. 5b) increased their expression in hBMSC pellets, especially in those from BECM expansion. In contrast, hBMSCs grown on UECM yielded pellets with an enhanced expression of Wnt11 (Fig. 5c) during chondrogenic induction compared with a decline in the groups preconditioned on either plastic or BECM, possibly indicating the active involvement of Wnt11 in UECM preconditioned hBMSC chondrogenic differentiation.

Discussion

USCs were first reported in 2008 and have been shown to have the ability to differentiate into cell lineages expressing urothelial, smooth muscle, endothelial and interstitial cell markers and, therefore, providing a potential cell source for urological tissue reconstruction (Zhang et al. 2008). In this study, we wished to determine whether hUSCs could differentiate into mesenchymal tissues, especially cartilage; we also wondered whether ECM deposited by hUSCs could contribute to the chondrogenic differentiation of stem cells. For the first time, we demonstrated that hUSCs are not able to differentiate into chondrocytes, despite the finding that hUSCs can differentiate into osteocytes, adipocytes and myocytes. ECM deposited by hUSCs can recharge senescent hBMSCs toward chondrogenic differentiation; ECM deposited by repeated-passage hBMSCs has a limited rejuvenation effect on expanded cells. The Wnt11-mediated noncanonical signaling pathway might be responsible for hUSC-deposited ECM-mediated hBMSC rejuvenation in terms of chondrogenic potential (see summary flowchart in Fig. 6).

Senescence-related issues are well known to prevent expanded cells from being clinically useful (Li et al. 2012). Our previous study showed that passage 5 hBMSCs can be rejuvenated after expansion on ECM deposited by passage 5 hBMSCs (Pei et al. 2011a). In this study, we found that passage 8 hBMSCs cannot be rejuvenated after expansion on ECM deposited by passage 8 hBMSCs. This finding suggests that replicative senescence might be the reason that hBMSCs lose their differentiation capacity (Vacanti et al. 2005) and that ECM loses its "stem cell cue" signals. Intriguingly, passage 8 hBMSCs can be rejuvenated after expansion on ECM deposited by hUSCs and are superior in chondrogenic capacity to passage 5 hBMSCs after expansion on ECM deposited by hBMSCs (Pei et al. 2011a), as evidenced by the ratio of GAG to DNA after 7-day chondrogenic induction (5.98±0.34 versus 3.62±0.80, $p=0.0032$), whereas hUSCs show no

Fig. 1 Characterization of human urine-derived stem cells (hUSCs). **a** ▶ Cell surface marker expression of hUSCs was detected by flow cytometry. Strongly positive markers (*i*): CD24, CD29, CD44, CD73, CD90, CD146 and SSEA-4. Weakly positive markers (*ii*): CD105, CD133 and STRO-1. Negatively expressed markers (*iii*): CD14, CD31, CD34, CD45 and CD117. The multi-differentiation potential of hUSCs in vitro was evaluated by using osteogenic, adipogenic and myogenic induction. **b** Osteogenic differentiation. Alizarin Red S staining for calcium deposition. **c** Adipogenic differentiation. Oil Red O staining for lipid droplets. **d**, **e** Myogenic differentiation. Immunofluorescent staining (*arrowheads*, *red*) for myogenic marker expression of Desmin and MyoD, respectively, in induced cells. *Bars* 50 μm. **f** Trophic factors secreted by hUSCs were analyzed by human cytokine enzyme-linked immunosorbent assay plate array and were mainly categorized as growth factors and immunomodulatory cytokines (*Adipo* adipokines, *FGF* fibroblast growth factor, *NGF* nerve growth factor, *EGF* epidermal growth factor, *G-CSF* granulocyte colony-stimulating factor, *IGF* insulin-like growth factor, *PAI* plasminogen activator inhibitor, *PDGF-BB* platelet-derived growth factor BB, *PLGF* placenta growth factor, *SCF* stem cell factor, *TGF* transforming growth factor, *VEGF* vascular endothelial growth factor, *GM-CSF* granulocyte/macrophage colony-stimulating factor, *IFN* interferon, *IL* interleukin, *IP* interferon-inducible protein, *MCP* monocyte chemoattractant protein, *MIP* macrophage inflammatory protein, *RANTES* regulated on activation, normal T cell expressed and secreted, *TNF* tumor necrosis factor)

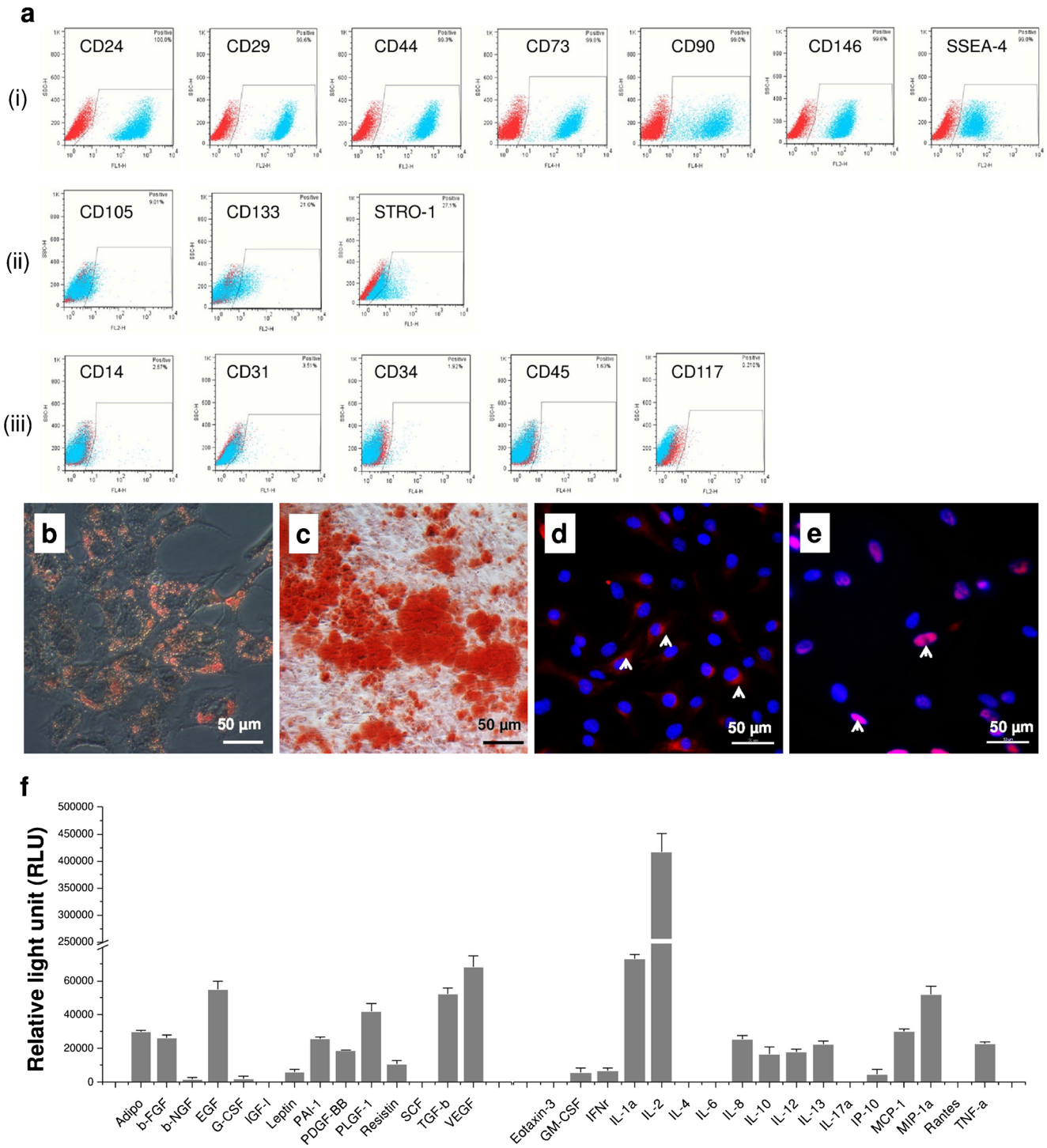

ability for differentiation into chondrocytes, even after expansion on ECM from each stem cell type, indicating that trophic effects from ECM deposited by hUSCs play a key role in rejuvenating senescent hBMSC chondrogenic potential. Type X collagen is concomitantly up-regulated at both the protein and mRNA levels in chondrogenically differentiated hBMSCs after expansion on ECM deposited by hUSCs, reminiscent of hBMSCs as a tissue-specific stem cell for endochondral ossification (Jones and Pei 2012; Pei et al. 2011a; Shen 2005).

By using the human cytokine ELISA plate array, we were able to detect the trophic factors released by hUSCs. The trophic factors detected in this study include various kinds of growth, inflammatory and immunomodulatory factors.

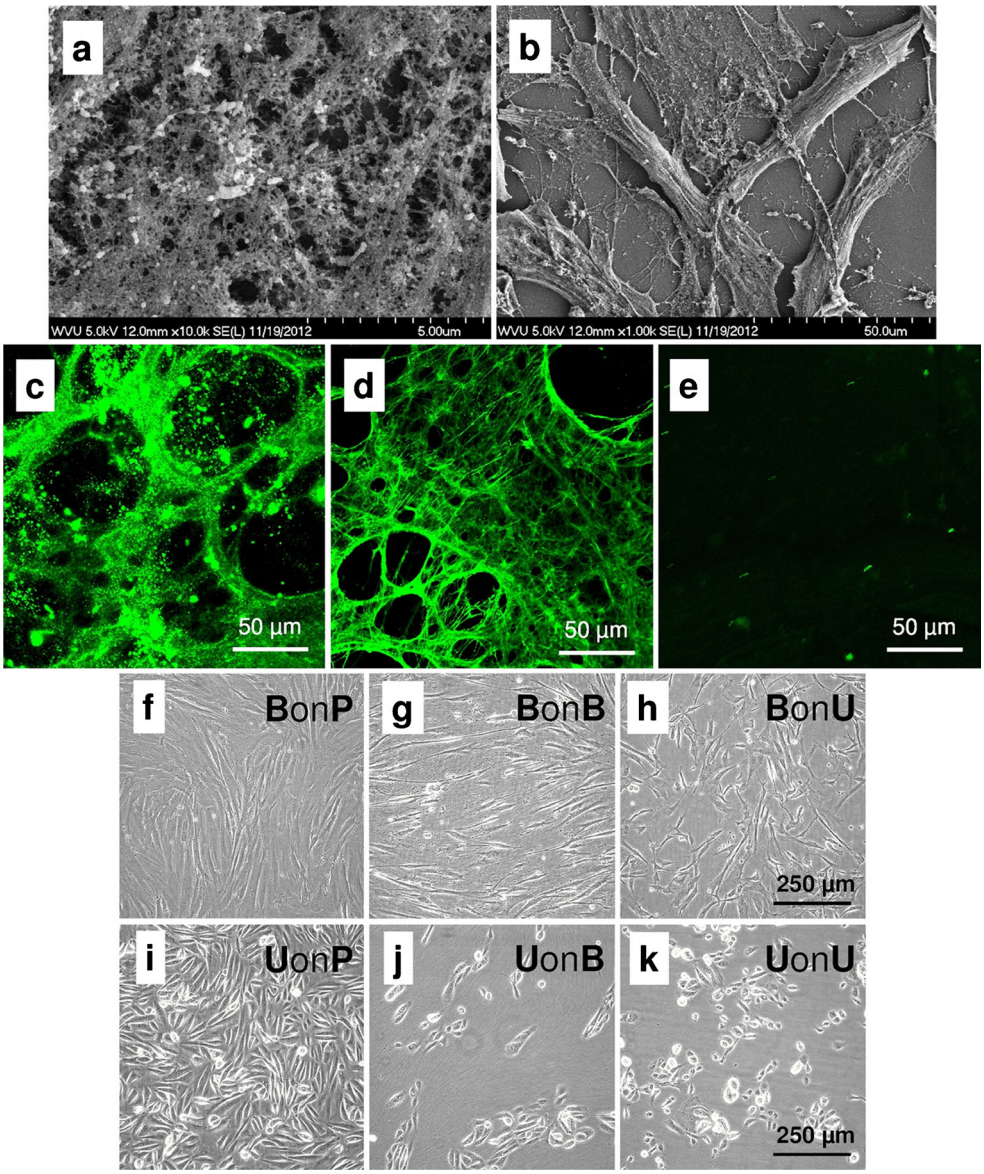

Fig. 2 Physicochemical properties of the extracellular matrix (ECM) deposited by hUSCs (UECM) and expanded cell morphology of hUSCs and human bone marrow stromal cells (hBMSCs). Scanning electron microscopy was used to observe (**a**) UECM and (**b**) hBMSCs grown on UECM. *Bars* 5 μm (**a**), 50 μm (**b**). Immunofluorescent staining was used to detect (**c**) type I collagen, (**d**) fibronectin, and (**e**) laminin 5. *Bars* 50 μm (**c**–**e**). Cell morphology after hBMSCs (**f** *BonP*, **g** *BonB*, **h** *BonU*) and hUSCs (**i** *UonP*, **j** *UonB*, **k** *UonU*) were expanded on plastic (*P*), BECM (*B* ECM from repeated-passage hBMSCs), or UECM (*U* ECM deposited by hUSCs) was examined by phase contrast microscope. *Bars* 250 μm (**f**–**k**)

In the growth factor category, the first deserving attention are VEGF-related factors consisting in VEGF, PLGF and PDGF. The formation of new vasculature is critical to regeneration and repair as both the driver and orientor of new bone formation. In this context, MSCs are proposed to be largely derived from pericytes associated with vasculature. A comprehensive perspective is presented in which signaling molecules such as PDGF take on new significance in vasculature-pericyte-MSC-osteoblast dynamics. Current data suggest that PDGF can function as a central connector between the cellular components and contributors of the osteoblast differentiation program. The inference is that PDGF acts at sites of injury to mobilize pericytes, to stimulate the mitotic expansion of these cells and to help organize them. In this way, PDGF both contributes to the osteogenic lineage and helps to stabilize newly forming vessels that drive the multistep multicomponent cascade of new bone formation (Caplan and Correa 2011). The second in the growth factor category are the adipo-related factors, such as Resistin, PAI-1, Leptin and Adipo. As adipose-derived stem cells show a reduced chondrogenic differentiation capacity under standard induction conditions (Sakaguchi et al. 2005; Winter et al. 2003), adipo-related properties might explain the undetectable chondrogenic capacity of the hUSCs in this study. The third category is that of anabolic growth factors, such as b-FGF, EGF and TGF-β. The FGFs play a central role during prenatal development and postnatal growth and regeneration of a wide variety of tissues, by promoting cellular proliferation and differentiation. All members of the FGF family bind, with varying degrees of affinity, to heparin sulfate proteoglycans, which serve as an extracellular storage site and, in some cases, appear to be involved in the activation of FGF receptors. EGF is a potent growth factor that stimulates the proliferation of various epidermal and epithelial cells. TGF-β is a protein that

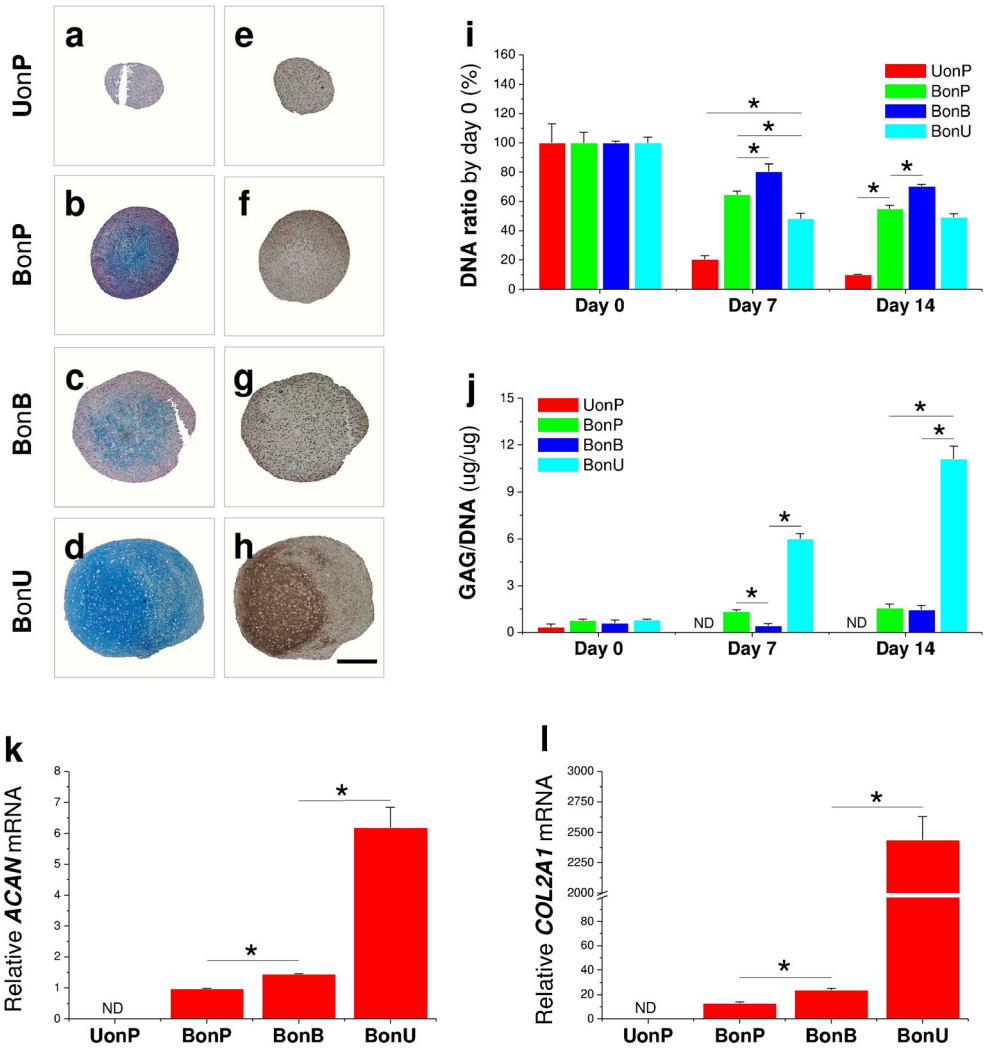

Fig. 3 Chondrogenic evaluation of expanded cells. After expansion on plastic, BECM, or UECM, the cells (hBMSCs or hUSCs) were cultured in a pellet system supplemented with a serum-free chondrogenic medium for 14 days (*UonP*, *BonP*, *BonB*, *BonU*). **a–d** Alcian blue staining to detect sulfated GAGs. **e–h** Immunohistochemical staining to detect type II collagen. *Bar* 800 μm. Biochemical analysis was used to measure the DNA and GAG amounts, which were used to calculate (**i**) the DNA ratio (cell viability) and (**j**) the ratio of GAG to DNA (chondrogenic index). TaqMan real-time PCR was used to evaluate (**k**) *ACAN* and (**l**) *COL2A1* mRNAs. **P*<0.05. Data are shown as averages ± SD for *n*=4

controls proliferation, cellular differentiation and other functions in most cells. Interestingly, IGF-I and SCF were not detectable in the released factors from hUSCs. The IGFs are mitogenic polypeptide growth factors that stimulate the proliferation and survival of various cell types including muscle, bone and cartilage tissue in vitro. Whether the lack of IGF-I release has any relationship with the undetectable chondrogenic differentiation in hUSCs is unknown.

The immunomodulatory factors include ILs, such as IL-2 and IL-12, cytokines, such as IFN and G-CSF and chemokines, such as MIP-1α. IL-2 is a powerful immunoregulatory lymphokine produced by T-cells in response to antigenic or mitogenic stimulation. By inducing IFNγ production by natural killer (NK) and T cells, IL-12 is a potent regulator of cell-mediated immune responses. Among its biological activities, IL-12 promotes the growth and activity of activated NK, CD4+ and CD8+ cells and induces the development of IFNγ-producing Th1 cells. IFNγ signaling in antigen-presenting cells and antigen-recognizing B and T lymphocytes regulates the antigen-specific phases of the immune response. Additionally, IFNγ stimulates a number of lymphoid cell functions including the anti-microbial and anti-tumor responses of macrophages, NK cells and neutrophils. G-CSF, a colony-stimulating factor hormone, is a glycoprotein, growth factor and cytokine produced by various tissues to stimulate the bone marrow to produce granulocytes and stem cells. MIP is crucial for immune responses to infection and inflammation (Ren et al. 2010).

In our study, hUSCs were not able to differentiate into chondrocytes, whereas immobilized trophic stimulation in the ECM deposited by hUSCs contributed to repeated-passage hBMSC chondrogenic potential, suggesting that paracrine actions of stem cells provide major beneficial effects in lieu of differentiation. The trophic factors secreted by stem cells can be delivered and might exert potential paracrine effects on other cell types through two approaches: soluble trophic factors in culture medium and immobilized trophic factors in ECM. The methods to isolate and concentrate stem-cell-conditioned media have been recently reported for harnessing the trophic factors produced by stem cells

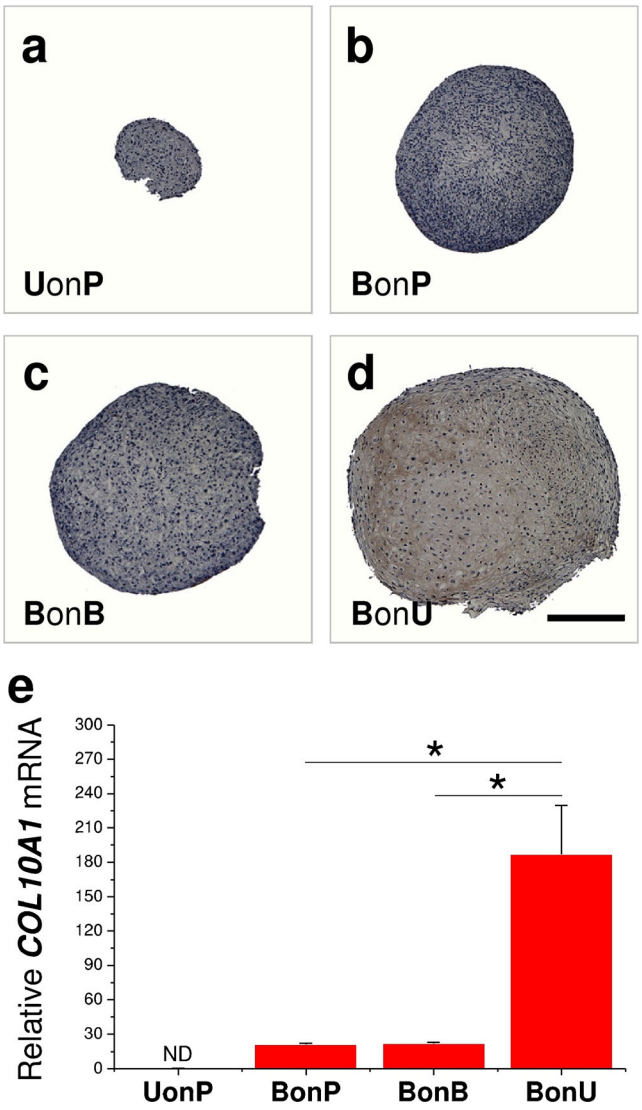

Fig. 4 Hypertrophic evaluation of expanded cells. After expansion on plastic, BECM, or UECM, the cells (hBMSCs or hUSCs) were cultured in a pellet system supplemented with a serum-free chondrogenic medium for 14 days (*UonP*, *BonP*, *BonB*, *BonU*). **a**–**d** Immunohistochemical staining was used to detect type X collagen. *Bar* 800 μm. **e** TaqMan real-time polymerase chain reaction was used to evaluate *COL10A1* mRNA. * $p<0.05$. Data are shown as averages ± SD for $n=4$ (*ND* not detectable)

(Gnecchi and Melo 2009). However, certain limitations exist for the therapeutic use of stem-cell-conditioned media; these include concerns about contamination by animal products, the in vitro half-lives of molecules secreted by stem cells and the relative amounts of secreted factors and the effective dosage necessary to elicit a functional response in vivo. In preparing our ECM, both deposited stem cells and stem-cell-conditioned media were removed, with the result that only the ECM remained. Since the matrix contains not only structural elements, such as collagens, laminins and fibronectin but also functional elements, such as FGF, PDGF, VEGF and TGF (Baraniak and McDevitt 2010), the exogenous administration of an ECM might catalyze tissue regeneration through the paracrine actions of morphogenic biomolecules sequestered within the matrix.

Since Wnt signaling is actively involved in TGF-β-mediated MSC chondrogenesis, we expected to observe a relationship between the chondrogenic potential of expanded hBMSCs after preconditioning and the Wnt signaling pathways. Wnt3a is known as a canonical Wnt protein, signaling through a β-catenin-dependent signaling pathway. Genetic deletion of β-catenin from early osteoprogenitors results in a lack of mature osteoblasts in the mouse embryo, whereas the forced activation of β-catenin greatly enhances osteogenesis (Rodda and McMahon 2006). On the contrary, Wnt3a mediates the inhibition of chondrogenesis in micromass cultures of embryonic chick limb-bud cells (Surmann-Schmitt et al. 2009). Wnt3a also strongly represses chondrogenesis and chondrocyte gene expression in cultured chondrocytic cells and differentiating limb-bud mesenchyme (Reinhold et al. 2006). In contrast to Wnt3a, Wnt5a and Wnt11 regulate cartilage-specific matrix molecules through a noncanonical pathway. Despite its function in regulating chondrogenesis, limb development and longitudinal skeletal outgrowth (Kawakami et al. 1999; Yang et al. 2003), the forced expression of Wnt5a delays chondrocyte maturation by inhibiting type X collagen expression, a marker for hypertrophic chondrocytes (Tufan and Tuan 2001). Thus, both Wnt3a and Wnt5a inhibit cartilage maturation; this might explain our data showing that 14-day chondrogenically differentiated hBMSCs in either the BECM or plastic expansion group exhibit higher expression of Wnt3a and Wnt5a but lower chondrogenic differentiation than the UECM expansion group. In the case of Wnt11, its expression is restricted to the prehypertrophic chondrocytes of the cartilage elements but it does not affect chondrogenic differentiation or hypertrophy of chondrocytes in chick micromass culture (Church et al. 2002; Loganathan et al. 2005). Wnt11 has been demonstrated to be capable of inhibiting canonical Wnt signaling through various intracellular pathways (Maye et al. 2004); this is consistent with our data that 14-day chondrogenically differentiated hBMSCs in the UECM expansion group displayed enhanced chondrogenic differentiation concomitantly with an up-regulation of Wnt11 expression. Our results are corroborated by a recent report that Wnt5a inhibits type II collagen expression by activating the c-Jun N-terminal kinase pathway, whereas Wnt11 enhances type II collagen expression by activating the protein kinase C signaling pathway. These data suggest that Wnt5a is associated with cartilage destruction, whereas Wnt11 plays a role in the maintenance of cartilage homeostasis (Ryu and Chun 2006).

In conclusion, we found that expansion on a matrix deposited by nonchondrogenic USCs strengthens the chondrogenic capacity of repeated-passage hBMSCs. We therefore believe USCs provide an excellent model for the

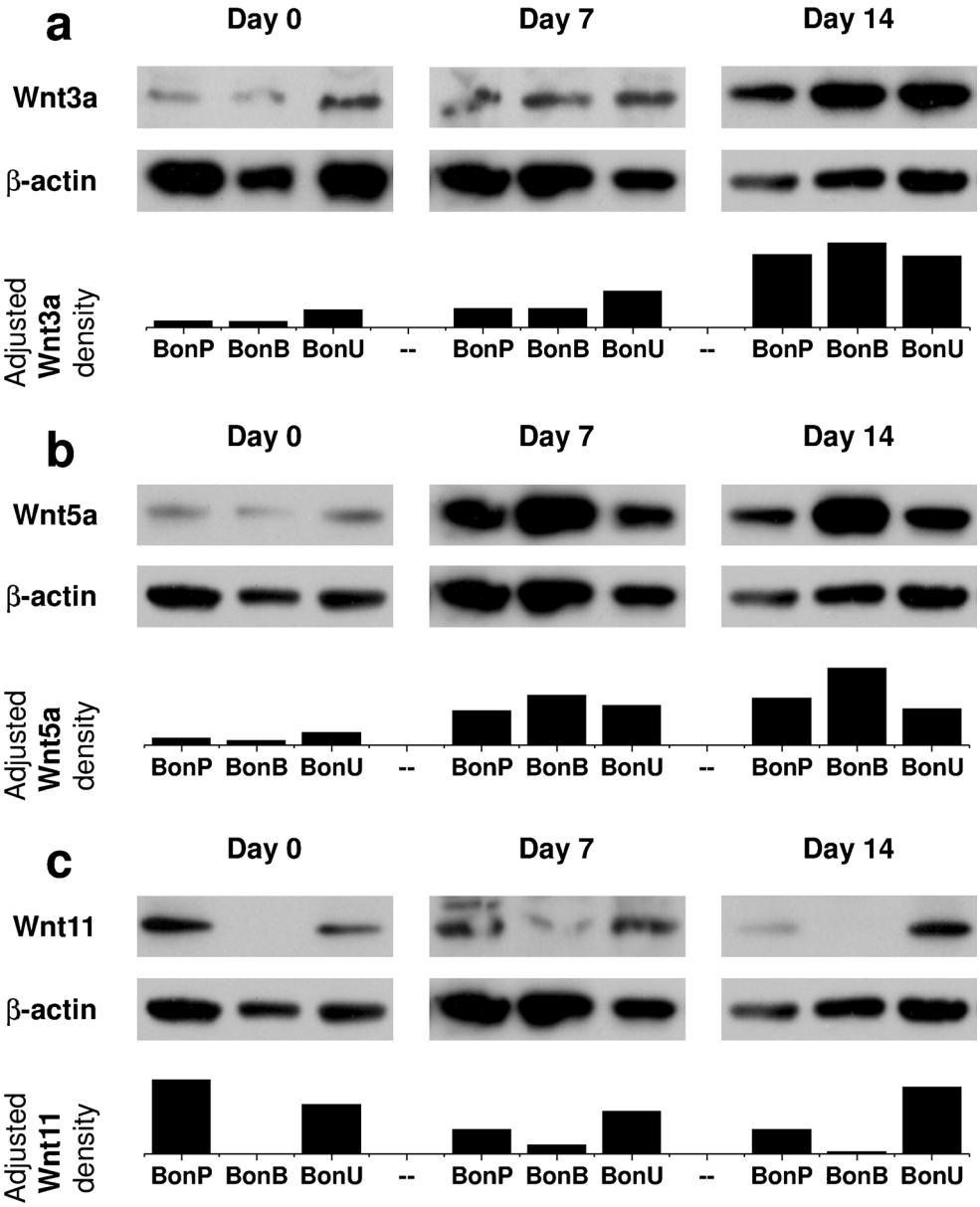

Fig. 5 Involvement of noncanonical Wnt signaling pathway during chondrogenic induction. Proteins were extracted from pellets of hBMSCs expanded on three substrates (*BonP*, *BonB*, *BonU*) and run on gels for Western blots. The pellets from hUSCs after expansion on plastic were too small to provide sufficient protein for this measurement. Canonical (**a** Wnt3a) and noncanonical (**b** Wnt5a, **c** Wnt11) Wnt signaling pathways were evaluated in chondrogenically differentiated hBMSCs at day 0 (condensation phase), day 7 (early phase of chondrogenic induction) and day 14 (late phase of chondrogenic induction). β-Actin served as an internal control. Image J software was used to semi-quantify immunoblotting bands

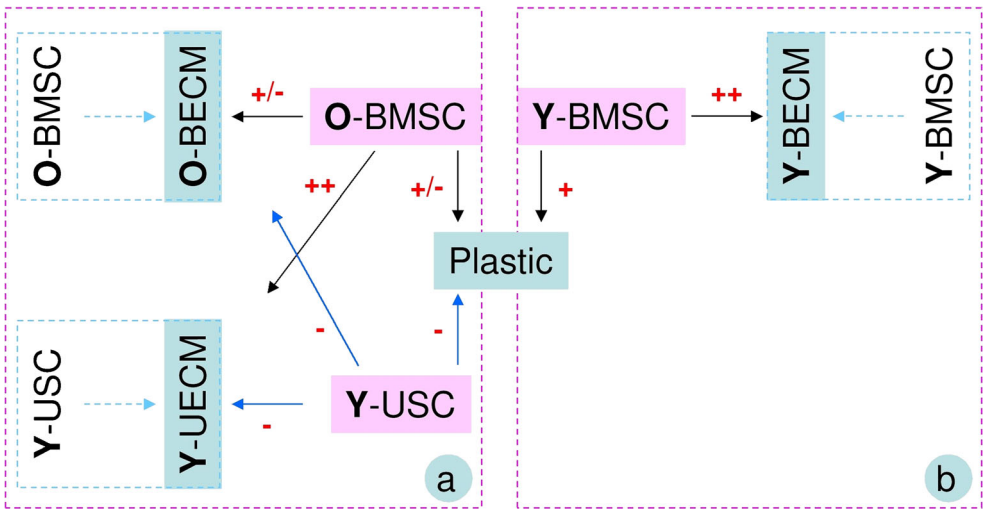

Fig. 6 Flow chart of a comparison (**a**) between young UECM (*Y-UECM*) and old BECM (*O-BECM*) from this study and of a comparison (**b**) between O-BECM and Y-BECM from a previous study (Pei et al. 2011a). Chondrogenic potential in either hBMSCs or hUSCs after expansion on plastic, BECM, or UECM was graded as strongly positive (+++), very positive (++), positive (+), positive/negative (+/−) and negative (−)

interpretation of the stem cell trophic effect, because this particular stem cell does not differentiate into chondrocytes, although its matrix contributes to the chondrogenic capacity of other stem cells. Expansion on UECM has also been found to be responsible for the up-regulation of Wnt11 in hBMSCs during subsequent chondrogenic induction. Gain-of-function and loss-of-function strategies will benefit further elucidation of the role of Wnt signals in ECM-mediated hBMSC rejuvenation. Despite the important findings of this study, some limitations deserve further investigation. For example, collagen, fibronectin and laminin are three major components of ECM (Dickinson et al. 2011); surprisingly, in the UECM, we detected type I collagen and fibronectin but no laminin 5. As is well known, laminins are major proteins in the basal lamina, the protein network foundation for most cells and organs with its influence on cell differentiation, migration, adhesion, phenotype and survival (Timpl et al. 1979). A comprehensive analysis of matrix components, such as the proteomics approach, is needed to uncover the rejuvenation effect of ECM on expanded cells. Despite the focus of this study on whether USCs contribute to cartilage regeneration, the effect of ECM rejuvenation on hBMSC proliferation, apoptosis, senescence and the cell cycle is also important and deserves more attention in future investigations.

Acknowledgement The authors thank Suzanne Danley for her help in editing the manuscript and Mark Shoukry for technical support.

Conflict of interest The authors declare no potential conflicts of interest.

References

Baraniak PR, McDevitt TC (2010) Stem cell paracrine actions and tissue regeneration. Regen Med 5:121–143

Caplan AI, Correa D (2011) PDGF in bone formation and regeneration: new insights into a novel mechanism involving MSCs. J Orthop Res 29:1795–1803

Church V, Nohno T, Linker C, Marcelle C, Francis-West P (2002) Wnt regulation of chondrocyte differentiation. J Cell Sci 115:4809–4818

Dickinson LE, Kusuma S, Gerecht S (2011) Reconstructing the differentiation niche of embryonic stem cells using biomaterials. Macromol Biosci 11:36–49

Djouad F, Bony C, Häupl T, Uzé G, Lahlou N, Louis-Plence P, Apparailly F, Canovas F, Rème T, Sany J, Jorgensen C, Noël D (2005) Transcriptional profiles discriminate bone marrow-derived and synovium-derived mesenchymal stem cells. Arthritis Res Ther 7: R1304–R1315

Gnecchi M, Melo LG (2009) Bone marrow-derived mesenchymal stem cells: isolation, expansion, characterization, viral transduction, and production of conditioned medium. Methods Mol Biol 482:281–294

He F, Chen XD, Pei M (2009) Reconstruction of an in vitro tissue-specific microenvironment to rejuvenate synovium-derived stem cells for cartilage tissue engineering. Tissue Eng Part A 15:3809–3821

Jo CH, Ahn HJ, Kim HJ, Seong S, Lee MC (2007) Surface characterization and chondrogenic differentiation of mesenchymal stromal cells derived from synovium. Cytotherapy 9:316–327

Jones B, Pei M (2012) Synovium-derived stem cells: a tissue-specific stem cell for cartilage tissue engineering and regeneration. Tissue Eng Part B Rev 18:301–311

Kawakami Y, Wada N, Nishimatsu SI, Ishikawa T, Noji S, Nohno T (1999) Involvement of Wnt-5a in chondrogenic pattern formation in the chick limb bud. Dev Growth Differ 41:29–40

Kronenberg HM (2003) Developmental regulation of the growth plate. Nature 423:332–336

Li JT, Pei M (2012) Cell senescence: a challenge in cartilage engineering and regeneration. Tissue Eng Part B 18:270–287

Li JT, Jones B, Zhang Y, Vinardell T, Pei M (2012) Low density expansion rescues human synovium-derived stem cells from replicative senescence. Drug Deliv Transl Res 2:363–374

Liu G, Pareta RA, Wu R, Shi Y, Zhou X, Liu H, Deng C, Sun X, Atala A, Opara EC, Zhang Y (2013) Skeletal myogenic differentiation of urine-derived stem cells and angiogenesis using microbeads loaded with growth factors. Biomaterials 34:1311–1326

Loganathan PG, Nimmagadda S, Huang R, Scaal M, Christ B (2005) Comparative analysis of the expression patterns of Wnts during chick limb development. Histochem Cell Biol 123:195–201

Maye P, Zheng J, Li L, Wu D (2004) Multiple mechanisms for Wnt11-mediated repression of the canonical Wnt signaling pathway. J Biol Chem 279:24659–24665

Pei M, He F, Kish V, Vunjak-Novakovic G (2008a) Engineering of functional cartilage tissue using stem cells from synovial lining: a preliminary study. Clin Orthop Relat Res 466:1880–1889

Pei M, He F, Vunjak-Novakovic G (2008b) Synovium-derived stem cell-based chondrogenesis. Differentiation 76:1044–1056

Pei M, He F, Kish VL (2011a) Expansion on extracellular matrix deposited by human bone marrow stromal cells facilitates stem cell proliferation and tissue-specific lineage potential. Tissue Eng Part A 17:3067–3076

Pei M, Li JT, Shoukry M, Zhang Y (2011b) A review of decellularized stem cell matrix: a novel cell expansion system for cartilage tissue engineering. Eur Cell Mater 22:333–343

Pei M, Zhang Y, Li JT, Chen DQ (2013) Antioxidation of decellularized stem cell matrix promotes human synovium-derived stem cell-based chondrogenesis. Stem Cells Dev 22:889–900

Reinhold MI, Kapadia RM, Liao Z, Naski MC (2006) The Wnt-inducible transcription factor Twist1 inhibits chondrogenesis. J Biol Chem 281:1381–1388

Ren M, Guo Q, Guo L, Lenz M, Qian F, Koenen RR, Xu H, Schilling AB, Weber C, Ye RD, Dinner AR, Tang WJ (2010) Polymerization of MIP-1 chemokine (CCL3 and CCL4) and clearance of MIP-1 by insulin-degrading enzyme. EMBO J 29:3952–3966

Rodda SJ, McMahon AP (2006) Distinct roles for Hedgehog and canonical Wnt signaling in specification, differentiation and maintenance of osteoblast progenitors. Development 133:3231–3244

Ryu JH, Chun JS (2006) Opposing roles of WNT-5A and WNT-11 in interleukin-1beta regulation of type II collagen expression in articular chondrocytes. J Biol Chem 281:22039–22047

Sakaguchi Y, Sekiya I, Yagishita K, Muneta T (2005) Comparison of human stem cells derived from various mesenchymal tissues: superiority of synovium as a cell source. Arthritis Rheum 52: 2521–2529

Shen G (2005) The role of type X collagen in facilitating and regulating endochondral ossification of articular cartilage. Orthod Craniofacial Res 8:11–17

Surmann-Schmitt C, Widmann N, Dietz U, Saeger B, Eitzinger N, Nakamura Y, Rattel M, Latham R, Hartmann C, von der Mark H, Schett G, von der Mark K, Stock M (2009) Wif-1 is expressed at cartilage-mesenchyme interfaces and impedes Wnt3a-mediated inhibition of chondrogenesis. J Cell Sci 122:3627–3637

Tan YB, Zhang YY, Pei M (2010) Meniscus reconstruction through co-culturing meniscus cells with synovium-derived stem cells on small intestinal submucosa. Tissue Eng Part A 16:67–79

Timpl R, Rohde H, Robey PG, Rennard SI, Foidart JM, Martin GR (1979) Laminin—a glycoprotein from basement membranes. J Biol Chem 254:9933–9937

Tufan AC, Tuan RS (2001) Wnt regulation of limb mesenchymal chondrogenesis is accompanied by altered N-cadherin-related functions. FASEB J 15:1436–1438

Vacanti V, Kong E, Suzuki G, Sato K, Canty JM, Lee T (2005) Phenotypic changes of adult porcine mesenchymal stem cells induced by prolonged passaging in culture. J Cell Physiol 205:194–201

Winter A, Breit S, Parsch D, Benz K, Steck E, Hauner H, Weber RM, Ewerbeck V, Richter W (2003) Cartilage-like gene expression in differentiated human stem cell spheroids: a comparison of bone marrow-derived and adipose tissue-derived stromal cells. Arthritis Rheum 48:418–429

Yang Y, Topol L, Lee H, Wu J (2003) Wnt5a and Wnt5b exhibit distinct activities in coordinating chondrocyte proliferation and differentiation. Development 130:1003–1015

Yates KE, Shortkroff S, Reish RG (2005) Wnt influence on chondrocyte differentiation and cartilage function. DNA Cell Biol 24:446–457

Zhang Y, McNeill E, Tian H, Soker S, Andersson KE, Yoo JJ, Atala A (2008) Urine derived cells are a potential source for urological tissue reconstruction. J Urol 180:2226–2233